Lossy Transmission Lines: Time Domain Formulation and Simulation Model

Patrick S. Yeung, *Member, IEEE*

***Abstract*— The time domain quasi-TEM equations for lossy transmission lines with R, L, C, and G parameters is reformulated and solved to relate directly the currents and voltages at the line terminations, at present and past times. This allows a computer model to be set up for simulating circuits with nonlinear terminations in the time domain using general circuit simulators. This formulation describes propagation of two dynamic forward and backward waves and is the extension of the method of characteristics to the lossy case. Distortion and impedance changes are generated by finite convolutions with past history information at the line terminations. For constant R, L, C, and G, and for a skin effect approximation, the kernels of Green's functions for these convolutions are derived as analytic expressions.**

I. Introduction

COMPUTER simulations of transmission line effects (signal delays, distortions, and crosstalk) have become an indispensible design tool for microwave, GaAs, and high-speed high-density digital circuit designs. These simulations must be accurate to act as software breadboards to help designers "get it right the first time." Nonlinear and frequency dependent effects need to be accounted for where appropriate, to ensure that the predicted simulation results correlate with the circuit performance after manufacture. This is especially important when design margins are tight and there is little room for overdesign.

Neglecting losses, transient analysis of transmission line networks with linear or nonlinear terminations is a well studied subject [1]. For lossy lines, several methods have been investigated [2]. Since nonlinear terminal networks are best analyzed in the time domain, recent developments focus on implementing a frequency domain analysis of the linear lossy line network in the nonlinear time domain solution. This is achieved by either the piecewise decomposition technique [3] or through time-domain Green's functions [4]. To be implemented in a general circuit simulator (such as SPICE, SCAMPER [5], or ASTAP [6]), the former approach requires nontrivial modifications to the matrix formulations of the simulator. On the other hand, the latter method in its present form suffers from the need for inserting negative impedance elements into the network and lengthy evaluations of Green's functions and their convolutions.

In this paper, we present an approach to analyze the lossy line directly in the time domain with the rest of the nonlinear network. We implement a time domain lossy line model in the general circuit simulator, in much the same manner as for lossless lines. This becomes possible after we formulate the time domain lossy line solution to relate directly the currents and voltages at the line terminations (at present and past times), as shown in (12). The Green's functions are square integrable and are analytic functions for constant R, L, C, and G parameters and for a skin effect approximation.

Manuscript received January 16, 1990; revised September 21, 1992.
The author was with Bell-Northern Research Ltd., Ottawa, Ont., Canada K1Y 4H7. He is now with INTELSAT, Washington, DC 20008.
IEEE Log Number 9208369.

II. Time Domain Formulation

In the quasi-TEM approximation [7], the standard frequency domain equations for a lossy transmission line are

$$\frac{\partial V(x,\omega)}{\partial x} + (R + j\omega L)I(x,\omega) = 0 \tag{1a}$$

$$\frac{\partial I(x,\omega)}{\partial x} + (G + j\omega C)V(x,\omega) = 0. \tag{1b}$$

The set of equations (1a) and (1b) is equivalent to the following:

$$\left[\frac{\partial}{\partial x} \pm \gamma(\omega)\right][V(x,\omega) \pm Z(\omega)\, I(x,\omega)] = 0 \tag{2a,b}$$

where

$$\gamma(\omega) = \sqrt{(R + j\omega L)(G + j\omega C)} \tag{2c}$$

and

$$Z(\omega) = \sqrt{(R + j\omega L)(G + j\omega C)^{-1}} \tag{2d}$$

The standard solution to (2) for a line of length d is

$$\begin{aligned}[V(0,\omega) &\pm Z(\omega)\, I(0,\omega)] \\ &= [V(d,\omega) \pm Z(\omega)\, I(d,\omega)] \exp\{\mp\gamma(\omega)d\}.\end{aligned} \tag{3}$$

For lossless lines, $\gamma(\omega) = j\omega\sqrt{LC}$ and $Z(\omega) = Z_0 = \sqrt{L/C}$. The time domain solution in this case, the Fourier transform of (3), relates the voltage and currents at the line terminations:

$$[\nu_{\text{out}}(t) + Z_0 i_{\text{out}}(t)] = [\nu_{\text{in}}(t-\tau) + Z_0 i_{\text{in}}(t-\tau)] \tag{4a}$$

$$[\nu_{\text{in}}(t) - Z_0 i_{\text{in}}(t)] = [\nu_{\text{out}}(t-\tau) - Z_0 i_{\text{out}}(t-\tau)] \tag{4b}$$

where $\nu_{\text{in}}(t) = \nu(0,t), \nu_{\text{out}}(t) = \nu(d,t), i_{\text{in}}(t) = i(0,t), i_{\text{out}}(t) = i(d,t)$, and the time delay is $\tau = d\sqrt{LC}$. Equation (4) forms the basis of the lossless line simulation model for general circuit simulators.

Figure 1 shows the equivalent circuit for the simulation model, using voltage sources. (This model may also be implemented using current sources.) During a time-domain analysis, the circuit simulator dynamically determines the time slices at which the analysis steps through. At each time slice, it solves for the voltages and currents which satisfy the circuit equations for the entire nonlinear circuit, based on information at past times. The transmission line model is primarily a subroutine enforcing (4) on the voltages and currents at the line terminations in the simulator solution.

In the case of lossy lines, the Fourier transform of the equation (2) or solution (3) is not normally defined, as the integrals are divergent. However, through careful handling of divergent terms, we are able to obtain equations with convergent expressions. Specifically, the divergences in $g(t)$ and $z(t)$, the Fourier transform of $\gamma(\omega)$ and $Z(\omega)$, respectively, are shown to be δ-function singularities:

$$g(t) = g_{\delta'}\delta'(t) + g_\delta \delta(t) + g_\epsilon(t)\,\epsilon(t) \tag{5a}$$

and

$$z(t) = z_\delta \delta(t) + z_\epsilon(t)\,\epsilon(t) \tag{5b}$$

where $\delta'(t)$ is the derivative of the δ-function and $\epsilon(t)$ is the Heaviside step function. We first derive the time domain equations and solution to set up the simulation model, delaying until Section IV to verify (5) and evaluate the expressions on the right-hand side.

The time domain equations are derived from the Fourier transform of (2) by using (5):

$$\left[\frac{\partial}{\partial x} \pm g_{\delta'}\frac{\partial}{\partial t} \pm \tilde{g}*\right] w_\pm(x,t) = 0 \tag{6a,b}$$

where

$$\tilde{g} = g_\delta + (g_\epsilon(t)\,\epsilon(t)) \tag{6c}$$

and $*$ defines the convolution operator with respect to t, so that

$$w_\pm(x,t) = \nu(x,t) \pm z * i(x,t) \tag{7a}$$

$$= \nu(x,t) \pm z_\delta i(x,t) \pm \int_{-\infty}^{t} z_\epsilon(t-t')\, i(x,t')\, dt'. \tag{7b}$$

In the convolution in (6), we have converted δ' in (5) into a time derivative on w and integrated the remaining δ-function terms.

The time domain solution is the transform of (3) (with $\tau = d\sqrt{LC}$):

$$w_\pm(x,t) = \tilde{k}(t,\tau) * w_\pm(x \mp d, t). \tag{8}$$

The Green's function $\tilde{k}(t,\tau)$ is given by the inverse Fourier transform

$$\tilde{k}(t,\tau) = \mathrm{FT}^{-1}\{\exp\left[-\gamma(\omega)d\right]\}. \tag{9}$$

This was evaluated before [8] for reflection-free infinitely long lines for constant $R, L, C,$ and G. For a general finite line with reflections, we solve (6) directly in the time domain in Section III and show that

$$\tilde{k}(t,\tau) = k(t-\tau,\tau) \tag{10a}$$

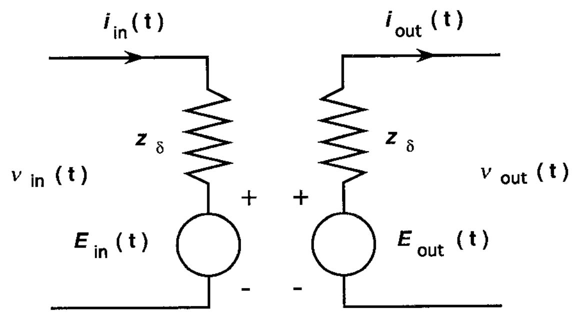

Fig. 1. Transmission line simulation model, where for lossless lines: $E_{\rm in}(t)$ = right-hand side of (4b), $E_{\rm out}(t)$ = right-hand side (4a). Lossy lines: $E_{\rm in}(t)$ = right-hand side of (12b) + $z_\epsilon * i_{\rm in}(t-\tau)$; $E_{\rm out}(t)$ = right-hand side of (12a) $- z_\epsilon * i_{\rm out}(t-\tau)$.

where

$$k(t,\tau) = k_\delta \delta(t) + k_\epsilon(t,\tau)\,\epsilon(t). \tag{10b}$$

Equation (8) becomes

$$w_\pm(x,t) = k(t,\tau) * w_\pm(x \mp d, t-\tau). \tag{11}$$

In terms of $\nu_{\rm in}(t), \nu_{\rm out}(t), i_{\rm in}(t),$ and $i_{\rm out}(t)$ defined before at the line terminations, the time domain solution (11)

$$w_{+,\rm out}(t) = k_\delta w_{+,\rm in}(t-\tau) + [k_\epsilon(t,\tau)\,\epsilon(t)] * w_{+,\rm in}(t-\tau) \tag{12a}$$

$$w_{-,\rm in}(t) = k_\delta w_{-,\rm out}(t-\tau) + [k_\epsilon(t,\tau)\,\epsilon(t)] * w_{-,\rm out}(t-\tau) \tag{12b}$$

where

$$w_{\pm,\rm out}(t) = \nu_{\rm out}(t) \pm z_\delta i_{\rm out}(t) \pm [z_\epsilon \epsilon(t)] * i_{\rm out}(t) \tag{12c}$$

and

$$w_{\pm,\rm in}(t) = \nu_{\rm in}(t) \pm z_\delta i_{\rm in}(t) \pm [z_\epsilon \epsilon(t)] * i_{\rm in}(t). \tag{12d}$$

Equation (12) relates the voltage and currents at the line terminations at time t with the history of voltages and currents, through convolution integrals with square-integrable kernels.

The lossy line model is set up as a subroutine enforcing (12) in place of (4) for the lossless case, as in Fig. 1. To evaluate (12), the line termination voltages and currents at past times in the simulator analysis are stored in memory. The convolution integrals are computed as matrix multiplications using a time discretization technique. Since the kernels are square integrable, we only need to evaluate the convolution integrals over a finite range, achieving significant speed improvements over previous formulations of the model [2]. For constant $R, L, C,$ and G, these kernels may be expressed as analytic functions, as is shown later. In addition, a model using current sources may be set up by swapping ν and i, z_ϵ^{-1} and $z_\epsilon, z_\delta^{-1}$ and z_δ in (11c–d), where $\mathrm{FT}(z_\epsilon^{-1}) = \{\mathrm{FT}(z_\epsilon)\}^{-1}$ and $z_\delta^{-1} = 1/z_\delta$.

Coupled line simulation model for a system of n lines may also be developed based on the above formulation. The quasi-TEM equations are given by (2) with $\gamma(\omega), Z(\omega), V(x,\omega),$

and $I(x,\omega)$, all promoted to $n \times n$ matrices [9]. In the cases where R, L, C, and G can be simultaneously diagonalized (e.g., mutually commuting) with frequency independent eigenvectors, the discussion in this paper applies to the diagonalized eigenmodes of propagation along lossy transmission lines. Examples are the even and odd modes for 2 coupled lines, and the case of symmetric equally spaced n-coupled lines with nearest neighbor coupling. For these cases, the simulation model is set up using congruence transformers [10].

For the general case, the matrix version of $\gamma(\omega)$ of (2) for n-coupled lines is diagonalized by a frequency dependent transformation matrix $\boldsymbol{S}(\omega)$. This transformation matrix and its inverse also relate elements of the vector $W_{\pm}(x,\omega) = V(x,\omega) \pm \boldsymbol{Z}(\omega)\boldsymbol{I}(x,\omega)$ with the eigenfunctions $W_{\pm,m}(x,\omega)$ which solve the diagonalized version of (2). Namely, $W_{\pm,m}(x,\omega)$ = the mth element of the vector $[\boldsymbol{S}(\omega)\, W_{\pm}(x,\omega)]$. In the time domain, these relations define the voltages $\nu(x,t)$ and currents $i(x,t)$ along the coupled lines as functions of the eigenfunctions $w_{\pm,m}(x,t)$ (i.e., the Fourier transform of $W_{\pm,m}(x,\omega)$), involving convolution integrals of $s(t)$, the Fourier transform of $\boldsymbol{S}(\omega)$, with $w_{\pm,m}(x,t)$. Inverse relations expressing $w_{\pm,m}(x,t)$ as functions of $\nu(x,t)$ and $i(x,t)$ are similarly derived, involving convolutions of $s^{-1}(t)$ with $w_{\pm}(x,t)$.

In the time domain coupled lines model, these relations among the line voltages, currents, and the eigenfunctions, evaluated at the line terminals at $x = 0$ and $x = d$, may be enforced via subroutines in each of two congruence transformer elements, interconnected by transmission lines corresponding to each of the eigenmodes. These transmission lines individually propagates one of the eigenfunctions according to equations (12) and are enforced as before in separate subroutines for each eigenmode. For the previous case of frequency independent $\boldsymbol{S}$, the convolution integrals to be evaluated in the congruence transformer elements reduce to simple matrix-vector multiplications, since the Fourier transform of $\boldsymbol{S}$ is a δ function.

III. Dynamic Traveling Waves

Equation (4) for lossless lines expresses an invariance condition. This is seen from the Fourier transform of (2a, b):

$$\left[\frac{\partial}{\partial x} \pm \sqrt{LC}\frac{\partial}{\partial t}\right][\nu(x,t) \pm Z_0 i(x,t)] = 0 \qquad \text{(13a,b)}$$

showing that $[\nu(x,t) \pm Z_0 i(x,t)]$ are constant along the forward (+) and backward (−) characteristics, $x \mp t/\sqrt{LC}$ = constant, corresponding to the forward and backward traveling waves.

For the lossy case, the integral-differential equations (6) describe propagation of dynamic forward and backward waves w_+, w_- (each carrying past history information) along the (±) characteristics. As they propagate, w_+ and w_- are distorted by the dynamic "sinks/sources" $\tilde{g} * w$ and modified internally by the dynamic impedance z_ϵ of (7). Indeed, (6) is the invariance condition (including sinks/sources) behind the simplicity of (12) and is the extension of the method of characteristics to the lossy case.

The Green's functions for the propagation of w is obtained by integrating (6). Any solution to (6) satisfies (for line length d)

$$\begin{aligned} w_{\pm}(x,t) &= \exp\left\{\mp d\left[\frac{\partial}{\partial x} \pm g_{\delta'}\frac{\partial}{\partial t} \pm \tilde{g}*\right]\right\} \\ &\quad \cdot w_{\pm}(x,t) && \text{(14a,b)} \\ &= \exp\{-d\tilde{g}*\}w_{\pm}(x \mp d, t-\tau) && \text{(14c,d)} \end{aligned}$$

where $\tau = dg_{\delta'}$ and $\exp\{s[\partial/\partial x \pm \sqrt{LC}\partial/\partial t]\}$ is the translation operator (i.e., $\exp\{s[\partial/\partial x \pm \sqrt{LC}\partial/\partial t]\}w(x,t) = w(x+s, t \pm s\sqrt{LC})$). In other words, the δ' singularity in $g(t)$ generate the time delay τ in $w_{\pm}$, and the δ-function term contributes to its attenuation.

Equating (14) to (11) we obtain $k(t,\tau)* = \exp\{-d\tilde{g}*\}$. Using the convolution theorem, we express $k(t,\tau)$ as

$$k(t,\tau) = \exp\{-g_\delta d\}\mathrm{FT}^{-1}[\exp\{-\gamma_\epsilon(\omega)d\}] \qquad \text{(15a)}$$

where

$$\gamma_\epsilon(\omega) = \mathrm{FT}\{(g_\epsilon(t)\,\epsilon(t))\}. \qquad \text{(15b)}$$

The divergent term in the FT^{-1} in (15) is extracted as in (10b), with

$$\begin{aligned} k_\delta(t,\tau)\,\delta(t) &= \exp\{-g_\delta d\}\mathrm{FT}^{-1}\{\exp[-\gamma_\epsilon(\infty)d]\} && \text{(16a)} \\ k_\epsilon(t,\tau)\,\epsilon(t) &= \exp\{-g_\delta d\}\mathrm{FT}^{-1} \\ &\quad \cdot \{\exp[-\gamma_\epsilon(\omega)d] - \exp[-\gamma_\epsilon(\infty)d]\} && \text{(16b)} \end{aligned}$$

For constant $R, L, C, G, \gamma_\epsilon(\infty) = 0$; hence, $k_\delta = \exp\{-g_\delta d\}$ and

$$\begin{aligned} k_\epsilon(t,\tau) &= b\tau\,\exp\{-a(t+\tau)\} \\ &\quad \cdot \frac{I_1(b\sqrt{(t+\tau)^2 - \tau^2})}{\sqrt{(t+\tau)^2-\tau^2}} \end{aligned} \qquad \text{(17)}$$

which is also obtained [8] from $\mathrm{FT}[\exp\{-\gamma(\omega)d\}]$, using (cf. (5))

$$\gamma_\epsilon(\omega) = \gamma(\omega) - g_\delta - j\omega g_{\delta'}. \qquad \text{(18)}$$

IV. Various Frequency Dependence

For constant R, L, C, G, we evaluated the functions in (5) to be

$$g_{\delta'} = \tau_0, \quad g_\delta = a\tau_0, \quad z_\delta = Z_0 \qquad \text{(19)}$$

$$g_\epsilon(t) = -\tau_0\left(\frac{b}{t}\right)\exp(-at)I_1(bt) \qquad \text{(20a)}$$

$$z_\epsilon(t) = Z_0 b\,\exp(-at)[I_1(bt) - I_0(bt)] \qquad \text{(20b)}$$

where

$$\begin{aligned} \tau_0 &= \sqrt{LC} \\ a &= \frac{1}{2}\left(\frac{R}{L} + \frac{G}{C}\right) \\ b &= \frac{1}{2}\left(\frac{G}{C} - \frac{R}{L}\right) \end{aligned} \qquad \text{(21)}$$

and I_0 and I_1 are the modified Bessel functions.

A method to obtain (19)–(21) is to observe that the transforms for $\gamma(\omega)$ and $Z(\omega)$ may be expressed formally as time derivatives of the inverse Fourier transform (FT^{-1}) of $\{1/\gamma(\omega)\}$, a finite function:

$$g(t) = \left(R + L\frac{\partial}{\partial t}\right)\left(G + C\frac{\partial}{\partial t}\right)\mathrm{FT}^{-1}\left\{\frac{1}{\gamma(\omega)}\right\} \quad (22a)$$

$$z(t) = \left(R + L\frac{\partial}{\partial t}\right)\mathrm{FT}^{-1}\left\{\frac{1}{\gamma(\omega)}\right\}. \quad (22b)$$

Explicitly,

$$\mathrm{FT}^{-1}\left\{\frac{1}{\gamma(\omega)}\right\} = [\exp(-at)I_0(bt)\,\epsilon(t)]. \quad (22c)$$

The derivatives of $\epsilon(t)$ in (22) yield $\delta(t)$ and $\delta'(t)$ in (5a) and (5b). Also, we have used the relations $I_0(0) = 1, I_1(0) = 0, I_0(bt)\,\delta'(t) = \delta'(t)$, and $\exp(-at)\delta'(t) = \delta'(t) + a\delta(t)$. Indeed, we recover 2(c–d) as the Fourier transform of (5) using (19)–(21).

For frequency dependent R, L, C, and G, the expressions for the singular and finite parts for $g(t)$ and $z(t)$ in (5) depend on the particular frequency behavior. First, to extract the singular terms, we observe that the divergent contributions come from the large ω region in the Fourier transform, resulting in a singularity at $t = 0$. Expanding $\gamma(\omega)$ and $Z(\omega)$ in positive and negative powers of ω, the singular terms may be identified by power counting inside the transform integral ($j\omega$ transforms into $\delta'(t)$, constant terms becomes $\delta(t)$ terms, and terms of $(1/j\omega)$ and higher orders are finite).

To be specific, the leading terms in ω for $\gamma(\omega)$ and $Z(\omega)$ are

$$\gamma(\omega) = j\omega\tau_0 + a\tau_0 - \frac{b^2\tau_0}{2j\omega} + \cdots \quad (23a)$$

$$Z(\omega) = Z_0 - \frac{bZ_0}{2j\omega} + \cdots. \quad (23b)$$

Here, τ_0, Z_0, a, and b are frequency dependent (cf. (21)), where the leading behavior of $\gamma(\omega)$ and $Z(\omega)$ are of order $j\omega$ and 1, respectively. The transform of (23) yields coefficients $g_{\delta'}, g_\delta$, and z_δ of (5). For example, the transform of $[j\omega\tau_0 + a\tau_0]$ in (23a) and Z_0 in (23b) yields the coefficients in (19) for constant R, L, C, and G.

The finite terms are obtained by subtracting the already identified singular terms from $g(t)$ and $z(t)$. This subtraction is performed in the frequency domain to obtain finite integrals. For constant R, L, C, and G, the transform of (18) defines the finite part g_ϵ using (19), and the transform of $[Z(\omega) - Z_0]$ from (23b) gives z_ϵ. As a quick check, the terms proportional to $1/j\omega$ in (23) reproduces the small t behavior of (20)–(21).

In the general case, causality restricts these finite terms to vanish for $t < 0$, i.e., they are of the form $g_\epsilon(t)\,\epsilon(t)$ and $z_\epsilon(t)\,\epsilon(t)$. The finite part of $k(t,\tau)$ is similarly restricted to be $k_\epsilon(t)\,\epsilon(t)$. Were they nonzero for $t > 0$, the convolution integrals in (12) would range over all values of t, and (12) would state that the currents and voltages at a particular time depend on what is to happen at future times. This imposes some restrictions on the type of frequency dependence of R, L, C, and G allowed for physical systems.

We discuss skin-effect losses as a second example. We assume constant L, C, G and approximate [11] $R = R_0 + R_1\sqrt{\omega}$. Substituting this expression for R into (23), and taking the transform, we obtain

$$\begin{aligned} g_{\delta'} &= \tau_0 \\ g_\delta &= a_0\tau_0 - j\frac{R_1^2\tau_0}{8L^2} \\ z_\delta &= Z_0 \end{aligned} \quad (24)$$

where a_0 is a of (21) with R set to R_0. The finite part $\gamma_\epsilon(\omega)$ is given by (18) where $\gamma(\omega)$ is obtained by setting $R = R_0 + R_1\sqrt{\omega}$ in (2c). Terms proportional to $\sqrt{\omega}$ and powers of $1/\sqrt{\omega}$ are included in the finite parts. The term Z_ϵ is obtained in a similar manner. If only the leading term in R_1 are kept in (2c,d) and $G = 0$, we obtain $k_\delta = 0$ and

$$\begin{aligned} k_\epsilon &= \exp(-a_0\tau_0 d)\frac{R_1 d}{4Z_0 t\sqrt{\pi t}}\exp\left(-\frac{R_1^2 d^2}{16Z_0^2 t}\right) \\ z_\epsilon &= \frac{1}{2\tau_0}\left[R_0 + \frac{R_1}{\sqrt{\pi t}}\right]. \end{aligned} \quad (25)$$

Whereas k_ϵ above leads to the results in [11] for reflectionless lines, (25) is only valid for $t \ll (L/R_1)^2$, since in this approximation, $\omega L \gg R_1\sqrt{\omega}$, or $\omega \gg (R_1/L)^2$. For large values of t corresponding to the small ω region where $R_0 \gg R_1\sqrt{\omega}$, (20) provides a good approximation. Furthermore, in the computer model, the small t region in the convolution integral in (12) must be handled correctly. Assuming w to be constant in the neighborhood $(t, t-\Delta)$, the integral of k_ϵ in this interval is $\exp(-a_0\tau_0 d)\,\mathrm{erfc}(R_1 d/4Z_0\Delta^{1/2})$, giving rise to a term in (12) similar to the k_δ term.

Finally, if there are no analytic expressions for k_ϵ and z_ϵ, the fast fourier transform method is used to evaluate (15) and (16) in the computer model. We need only to compute this initially before the transient analysis. Furthermore, since the large ω divergences have already been taken out, the computation is fast.

V. Simulation Results

The lossy line model described above has been implemented in SCAMPER [5], which allows modeling through user defined Fortran subroutines. This model deals with the lossless line as a special case (where convolutions are unnecessary), since (12) goes over smoothly into (4) when $R = G = 0$. Various lossless results are easily recovered.

As an example to verify the lossy aspects of the model, we simulated a nonlinear network of a linear source driving a transmission line with a nonlinear load. The source has output resistance and capacitance of 75 Ω and 2 pF, respectively, the transmission line is characterized by $R = 75\,\Omega$/m, $G = 0.01$ mho/m, $Z_0 = 40\,\Omega, \tau = 2$ ns, and $d = 50$ cm. The load has an input C–L–C stage with capacitances C and inductance L of 2 pF and 10 nH, respectively, connected to a resistance of 75 Ω in series with a nonlinear element in which the current is proportional to the square of the voltage across the nodes ($I = 10^{-4}\,\mathrm{V}^2$). The simulated circuit response was very close to that obtained using the method of [3].

In a more practical application, we simulated a circuit consisting of a high speed CMOS driver–receiver pair connected by a line with $R = 40\,\Omega$/m, $G = 0.02$ mho/m,

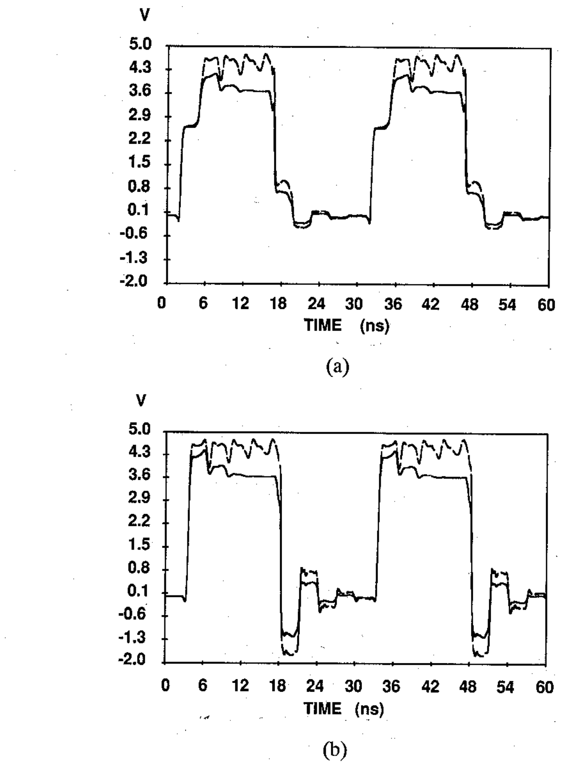

Fig. 2. (a) Voltage at driver end. (b) Voltage at receiver end. ---- lossless line; — lossy line.

$Z_0 = 35\,\Omega, \tau = 0.85$ ns, and $d = 12$ cm. The driver and receiver models together have 28 active nonlinear transistors. The results at the near and far ends are shown in Fig. 2, where the lossless case is also displayed as a comparison. For lossy lines, the simulator spends more time at each time-slice to evaluate the convolution integrals. This is, however, offset by the fewer analysis iterations needed by the simulator in this case, which has a smoother waveform since ringing is damped. CPU time for this complex example for 2 periods is 1.7 min on an IBM 3090-200E, demonstrating the practicality of this method (lossless case and the case of a short between driver and receiver were 15% and 35% faster, respectively).

VI. Conclusions

We have presented a new formulation of the time domain lossy line equations, which describe separate propagation of dynamic forward and backward waves. The solution relates currents and voltages at the line terminations at present and past times, involving convolutions with past history information. For constant R, L, C, G, we evaluated the Green's functions in terms of modified Bessel functions. For frequency dependent R, L, C, G, we described how to obtain finite expressions, giving as an example the kernels in a skin effect approximation. Based on this solution, we set up the time domain lossy line simulation model. This model is efficient because it builds on the robustness of the familiar lossless model, and because the square integrable Green's functions provide an effective natural cutoff for the required convolution integrals. Transmission line networks with existing nonlinear device models are simulated easily in the lossy case, as shown in an example.

References

[1] F. H. Branin, "Transient analysis of lossless transmission line," *Proc. IEEE,* vol. 55, no. 11, pp. 11012–1013, Nov. 1967.

[2] A. R. Djordjevic, T. K. Sarkar, and R. F. Harrington, "Time domain response of multiconductor transmission lines," *Proc. IEEE,* vol. 75, pp. 743–746, June 1987.

[3] M. S. Nakhla, "A piecewise decomposition technique for analysis of nonlinear networks with distributed components," *Proc. 22nd IEEE Int. Symp. Circuit Syst.,* 1989, pp. 606–609.

[4] A. R. Djordjevic, T. K. Sarkar, and R. F. Harrington, "Analysis of lossy transmission lines with arbitrary nonlinear terminal networks," *IEEE Trans. Microwave Theory Tech.,* vol. MTT-34, pp. 660–666, June 1986.

[5] D. Agnew, "SCAMPER: Circuit design tool for 1980's," *Telesis* (Bell-Northern research publication), no. 3, pp. 2–9, 1980.

[6] IBM, "Advanced statistical analysis program," in-house circuit simulator.

[7] S. A. Schelkunoff, "Conversion of Maxwell's equations into generalized telegraphist's equations," *Bell Syst. Tech. J.,* vol. 34, pp. 995–1043, Sept. 1955; J. Chilo, C. Moullor, and M. Bouthimon, "Interconnection effects in fast logic integrated GaAs circuits," *Int. J. Electron.,* vol. 58, pp. 671–686.

[8] E. Weber, *Linear Transient Analysis,* vol. 2. New York: Wiley, 1956, p. 383. Preis, D. "Pulse dispersion and dissipation in very-high-speed integrated circuits," in *IEEE Proc. Int. Symp. Circuits Systems,* 1983, pp. 1358–1362; C. V. Gura and J. A. Abraham, "Improved methods of simulating *RLC* coupled and uncoupled transmission lines based on the method of characteristics," in *Proc. 25th IEEE DAC,* 1988, pp. 300–305.

[9] A. J. Gruodis and C. S. Chang, "Coupled lossy transmission line characterization and simulation," *IBM J. Res. Develop.,* vol. 25, pp. 25–41, Jan. 1981, and references therein. See also [2].

[10] F. Y. Chang, "Transient analysis of lossless coupled transmission lines in a nonhomogeneous dielectric medium," *IEEE Trans. Microwave Theory Tech.,* vol. MTT-18, pp. 616–626, Sept. 1970.

[11] C. S. Chang, "Electrical design of signal lines for multilayer printed circuit boards," *IBM J. Res. Develop.,* vol. 32, pp. 647–657, Sept. 1988.

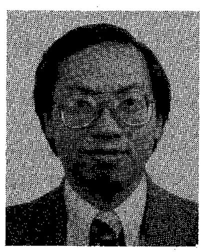

Patrick S. Yeung (M'86) received the B.A. degree in 1972 and Ph.D. degree in 1977, from Princeton University and M.I.T. respectively, both in physics.

From 1977 to 1980, he was a Lecturer at M.I.T. After 1980 he was a Lecturer at McGill University. In 1983, he joined Bell-Northern Research as a Member of the Scientific Staff, and in 1985 became Manager for a design simulation and analysis group developing design tools in electromagnetic, analog, digital, and reliability simulations, as well as telecommunication high-speed switching product design support. Since 1990, he has been with the Research and Development Department of the International Telecommunications Satellite Organization (INTELSAT), Washington, D.C., where he is involved with developing new technologies for future satellites.